Wear Testing/Materialography

Tanju Teker*, S. Osman Yilmaz and İ. Savaş Dalmiş

Effect of FeTi-FeB inoculation on the shape of carbide reinforcements in hypoeutectic high chromium white cast iron

https://doi.org/10.1515/mt-2021-2047

Abstract: FeTi-FeB was added to molten high chromium white cast iron in amounts of 0.5–2.5 wt% at 50 °C above the melting temperature. The samples were produced in four groups. The first group samples were investigated as cast, the second group homogenized at 1000 °C for 1 h, and the other two groups were also homogenized at 1000 °C but for 3 and 6 h, respectively. To study the effect of FeB and FeTi on the microstructure, the samples were characterized by optical microscopy, scanning electron microscopy, energy dispersive spectroscopy, X-ray diffraction and hardness tests. Wear tests were performed using a pin-on disc. A homogeneously dispersed carbide microstructure was produced by the homogenization heat treatment method. The addition of FeTi-FeB inoculants to high Cr white cast iron played an important role in the distribution of hard carbides. The chemical rate and the carbide volume varied on account of the added hard inoculant particles. TiB_2, Cr_3C_2, M_7C_3, $M_{23}C_6$, and γ-FeCr phases formed on the surfaces. The hardness and wear resistance were improved considerably due to FeTi-B inoculation.

Keywords: FeB; FeTi; heat treatment; inoculation; microstructure; white cast iron.

1 Introduction

Materials with high chromium white cast iron (HCrWCI) are widely utilized in various industries including mining processes and cement manufacturing. These alloys are used to process hard materials such as cement, gravel etc. The materials have high wear resistance due to hard carbides. The austenite matrix structure is the most commonly observed in high chrome alloys. There are M_7C_3 carbide structures in these alloys. M_7C_3 carbide types grow as blades and bars parallel to the direction of heat flow in the long axis of the mold [1–4]. Wear resistance depends on the chemical compound, process conditions and heat treatment. Such alloy systems should be determined according to these parameters in addition to the tribological environment. Significant microstructural parameters on wear performance are the carbide volume, morphologic structure of the carbides, and the interface between the matrix and the hard carbide phases [5–7]. These parameters can also play a significant role in the hardness and fracture toughness. In addition, the microstructures of white cast iron and metal matrix composites have many similarities. According to the temperature at which the particles are inoculated into the melt, composites with externally added particles have two types of foundry methods. The particles are inoculated above the liquid temperature in the liquid metallurgical process. There are many parameters affecting the final product such as wettability that can affect the type of particles, shape, surface, size, roughness and alloying elements in the melt, surface chemistry of the outer atomic layers and the gas environment of the particles. The discontinuous reinforcement phase composites are widely used due to their availability, low cost, independent particle orientation and ease of production [8–10]. Titanium (Ti) is an important carbide and boride former. Titanium carbide and titanium diborides have high hardness values. There are high tensile strength values and high resistance to wear at high temperatures in titanium carbide and titanium diborides, which means high elasticity module and compressive strength [11–13]. Scandian et al. reported the effect of chromium and molybdenum rates in different proportions on the wear behavior of white cast iron. Matrix morphology and carbide shape depend on the amount of Mo and Cr [14]. Mohammadnezhad et al. researched the influence of Va on the microstructure, hardness, toughness of Ni-Hard4 WCI. The addition of Va

***Corresponding author: Tanju Teker**, Department of Manufacturing Engineering, Faculty of Technology, University of Sivas Cumhuriyet, 58140, Sivas, Turkey, E-mail: tanjuteker@cumhuriyet.edu.tr
S. Osman Yilmaz and İ. Savaş Dalmiş, Faculty of Engineering, Department of Machine Engineering, University of Namık Kemal, 59500, Çorlu, Tekirdağ, Turkey

Table 1: Chemical compositions of the inoculant particulates (wt%).

Elements	Fe	Ti	Si	S	Al	B	C	P
FeTi	Bal.	75	0.5	0.03	4.5	–	0.3	0.03
FeB	Bal.	–	0.4	0.05	3.4	16	–	0.04

improved the hardness and wear of Ni-Hard4 [15]. Xiaohui et al. reported the effect of Nb on the microstructure and mechanical performance of HCrCI. The carbides became thinner and the M_7C_3 carbides changed to isotropic [16].

This study aimed to produce hypoeutectic high chromium white cast iron inoculated by FeTi-FeB to create spherical hard carbide reinforcements in the microstructure.

2 Experimental procedure

FeB and FeTi inoculant particles of 150 (µm) and high chromium white cast iron were selected as study materials. FeB and FeTi particles was added to molten high chromium white cast iron in amounts of 0.5–2.5 wt% at 50 °C above the melting temperature. The chemical composition of the inoculant particles is given in Table 1. Chemical properties and heat treatments are presented in Table 2. The samples were produced in four groups. The first group samples were investigated as cast, the second group homogenized at 1000 °C for 1 h, and the other two groups were also homogenized at 1000 °C but for 3 and 6 h, respectively. Samples were subjected to air-cooling. For metallographic examination, samples were ground and polished, then etched with a solution of 5 g $FeCl_3$, 30 ml HCl and 100 ml distilled water. To study the effect of FeTi and FeB on the microstructure, the samples were characterized by optical microscopy (LEICA DM750), scanning electron microscopy (SEM: ZEISS EVO LS10) and energy dispersive spectroscopy (EDS), X-ray diffraction (XRD: Bruker), and hardness tests (QNESS Q10: HV and HRC scale). Wear tests were performed using a pin-on disc under 30 N load.

3 Results and discussion

3.1 Evaluation of the microstructure

The microstructures of the S1 group without inoculation are given in Figure 1a–d. The microstructure of white cast iron varied considerably according to the chemical composition.

Table 2: Chemical compositions and heat treatment of the samples.

Chemical composition (wt%)								
Sample no	**C**	**Mn**	**Si**	**Mo**	**Cr**	**Cu**	**FeTi + FeB**	**Heat treatment**
S1.1	3.01	0.27	2.02	1.33	26.48	0.13	–	As cast
S1.2	3.01	0.27	2.02	1.33	26.48	0.13	–	1000 °C, 1 h
S1.3	3.01	0.27	2.02	1.33	26.48	0.13	–	1000 °C, 3 h
S1.4	3.01	0.27	2.02	1.33	26.48	0.13	–	1000 °C, 6 h
S2.1	2.95	0.27	2.02	1.43	26.42	0.13	0.5	As cast
S2.2	2.95	0.27	2.02	1.43	26.42	0.13	0.5	1000 °C, 1 h
S2.3	2.95	0.27	2.02	1.43	26.42	0.13	0.5	1000 °C, 3 h
S2.4	2.95	0.27	2.02	1.43	26.42	0.13	0.5	1000 °C, 6 h
S3.1	3.07	0.56	1.96	1.32	26.47	0.2	1	As cast
S3.2	3.07	0.56	1.96	1.32	26.47	0.2	1	1000 °C, 1 h
S3.3	3.07	0.56	1.96	1.32	26.47	0.2	1	1000 °C, 3 h
S3.4	3.07	0.56	1.96	1.32	26.47	0.2	1	1000 °C, 6 h
S4.1	3.09	0.56	1.76	1.36	25.76	0.2	1.5	As cast
S4.1	3.09	0.56	1.76	1.36	25.76	0.2	1.5	1000 °C, 1 h
S4.1	3.09	0.56	1.76	1.36	25.76	0.2	1.5	1000 °C, 3 h
S4.1	3.09	0.56	1.76	1.36	25.76	0.2	1.5	1000 °C, 6 h
S5.1	2.96	0.56	2.24	1.58	25.37	0.20	2	As cast
S5.2	2.96	0.56	2.24	1.58	25.37	0.20	2	1000 °C, 1 h
S5.3	2.96	0.56	2.24	1.58	25.37	0.20	2	1000 °C, 3 h
S5.4	2.96	0.56	2.24	1.58	25.37	0.20	2	1000 °C, 6 h
S6.1	3.04	0.64	1.97	1.16	26.32	0.11	2.5	As cast
S6.2	3.04	0.64	1.97	1.16	26.32	0.11	2.5	1000 °C, 1 h
S6.3	3.04	0.64	1.97	1.16	26.32	0.11	2.5	1000 °C, 3 h
S6.4	3.04	0.64	1.97	1.16	26.32	0.11	2.5	1000 °C, 6 h

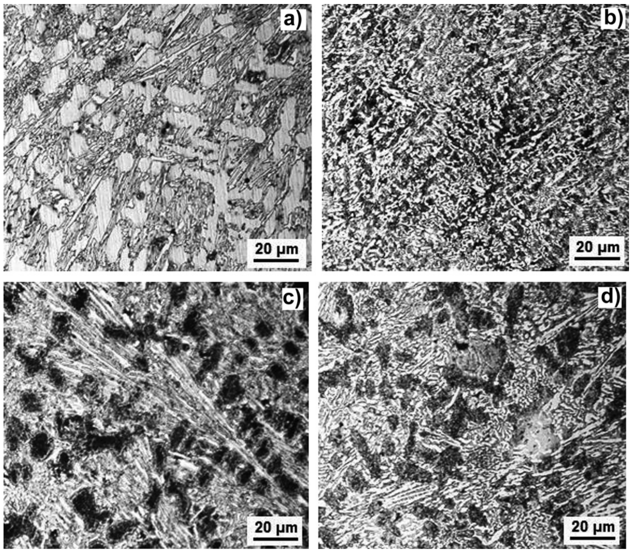

Figure 1: Optic microscopy images of samples, a) $S_{1.1}$, b) $S_{1.2}$, c) $S_{1.3}$, d) $S_{1.4}$.

Samples having 27 wt% chrome consisted of an austenitic matrix and M_7C_3 carbide types. The microstructure had pro-eutectic austenite dendrites and eutectic cells formed from M_7C_3 carbides and an austenite phase as the cast form (Sample $S_{1.1}$). Heat treatment dissolved large pro-eutectic austenite phase dendrites in the microstructure of sample $S_{1.2}$ in Figure 1b. M_7C_3 carbides with irregular size distribution were predominant, and the structure was transformed into eutectic cells (γ + M_7C_3) formed through the remaining microstructure. Carbides in sample $S_{1.1}$ had rod-like carbides structure together with blade-type morphology. Moreover, blade-like carbides generally occurred around the large pro-eutectic M_7C_3 carbides. From the heat treatment results, it can be seen that the austenite size reduced and austenite decomposition dissolved M_7C_3 carbide.

M_7C_3 carbide formation had many different physical forms regarding the zone of solidification. The existence of a eutectic cell prevented the growth of carbide. Also, there were thin carbides in the hypoeutectic cast iron structures and they had two types of carbides (Figure 1). Large-shaped carbides had dendritic physical form, and small secondary carbides of less than 1 (µm) were deposited in the particles. The carbides were seen to form on the surface of the sand casting (max. 5 mm) perpendicular to the surface. The carbides in the cast were generated randomly. It was found that the carbide type (hypoeutectic) in samples with carbides of less than 20 wt% had blade-type M_7C_3 carbides because of the eutectic liquid between dendrites (Figure 1a). The dendritic form of the primary carbides was altered, and the size of the carbides was reduced with heat treatment (Figure 1b–d). The M_7C_3 carbide core was removed before the temperature of the peritectic reaction was reached. Thus, the pro-eutectic M_7C_3 carbides could not react with the liquid phase to form core and rim structures. Therefore, the addition of titanium before casting accelerated pro-eutectic M_7C_3 carbide nucleation, the eutectic formation from austenite, and M_7C_3 carbide type from the liquid phase. Increasing the FeTiB inoculation concentration increased the amount of TiB_2. X-ray diffraction results of samples $S_{1.1}$ and $S_{6.1}$ are shown in Figure 2a and b. It was understood from the X-ray analysis results that TiB_2 and M_7C_3 phases occurred in the microstructure. Depending on the number of additive inoculations, the volume of TiB_2 phases changed in the structure. This phase had a hard structure, low density, high Young's modulus, and high melting temperature. In addition, there was a tetragonal structure with good strength properties. This phase was beneficial for abrasive wear resistance applications [12–14].

Four groups of samples were manufactured with differing rates of inoculation. The size and microhardness of the carbides changed due to inoculation volume. Borides and carbides decomposed up to 1600 °C, and throughout solidification, the TiB_2 and a solid solution of (Ti, Cr, Mo)B_2 occurred depending on increasing solubility of molybdenum and chrome. The metallographic examinations of all

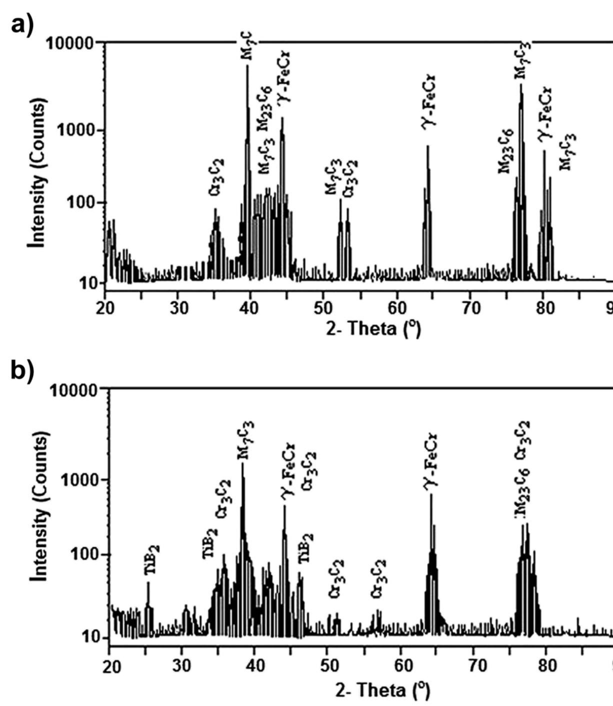

Figure 2: X-ray diffraction of sample, a) $S_{1.1}$, b) $S_{6.1}$.

samples revealed that the hard particles were non-uniformly dispersed in the matrix structure because of the differences of density between the externally added particles and the molten matrix. The morphology of carbide in high chromium white cast iron is formed from rod and blade-like structures. It was confirmed that the rod and blade structure growth occurred in hypoeutectic and eutectic irons. The adjacent hypoeutectic rod growth in the melt limited the length of a hypoeutectic rod. Due to the microstructure, the micro-hardness of the carbides and energy dispersive spectroscopy analysis, hypo-centric carbides are thought to form throughout solidification (Figure 3). EDS analysis of Sample $S_{2.1}$ is shown in Figure 3 and Table 3.

However, inoculation of pure Ti did not give the desired structure because of the density difference between titanium and iron and titanium's affinity to oxygen (and its propensity to form TiO_2). Thus, titanium was added as the FeTiB phase former. The results showed that precipitated TiB_2 was not formed. Therefore, heat treatment was carried out for secondary carbide and boride precipitation. The influences of the heat treatment on $S_{2.1}$, $S_{2.2}$, $S_{2.3}$, and $S_{2.4}$ samples are indicated in Figure 4.

The rate of FeTiB was gradually increased to 0.5, 1.0, 1.5, 2.0 and 2.5 wt%. The resulting microstructures revealed that these particles added to the microstructure affected the eutectic phase and primary carbides formed for nucleation sites throughout solidification in the hypoeutectic region. The microstructures of $S_{3.1}$, $S_{3.2}$, $S_{3.3}$, and $S_{3.4}$ samples are illustrated in Figure 5. Significant numbers of titanium-containing pro-eutectic carbides were observed. From the microstructure, the particles that were added throughout casting were found to act as nucleation

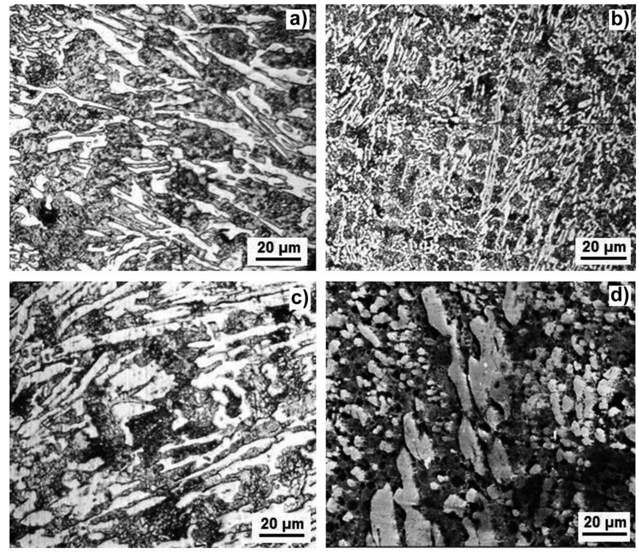

Figure 4: OM and SEM micrographs of samples, a) $S_{2.1}$, b) $S_{2.2}$, c) $S_{2.3}$, d) $S_{2.4}$.

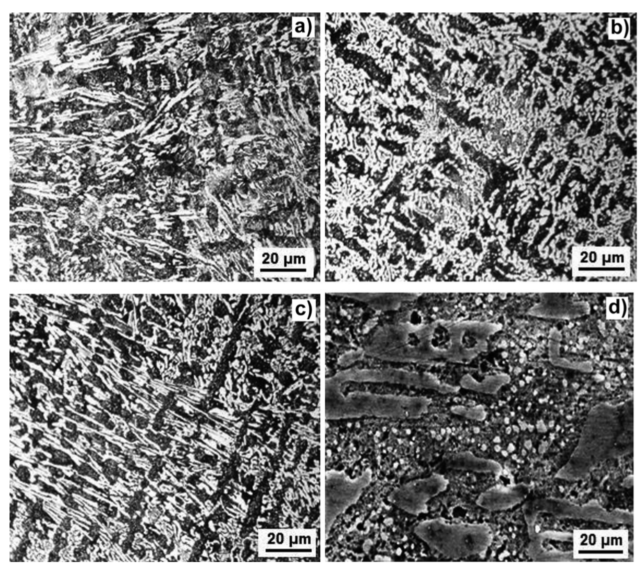

Figure 5: OM and SEM micrographs of samples, a) $S_{3.1}$, b) $S_{3.2}$, c) $S_{3.3}$, d) $S_{3.4}$.

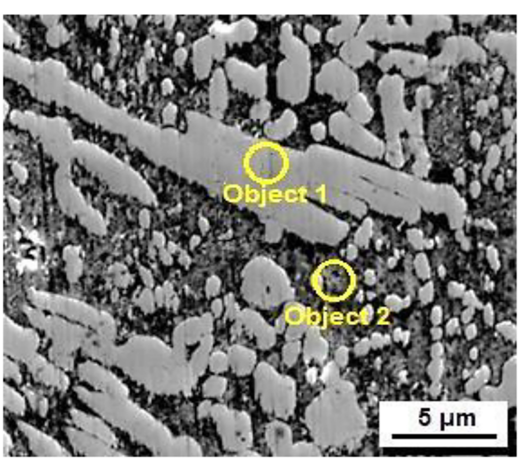

Figure 3: EDS analysis spectrums of sample $S_{2.1}$.

Table 3: EDS analysis results of sample $S_{2.1}$ (wt%).

Elements	Cr	Fe	C	Mn	Ni	Al	Ti	V	Si
Object 1	45.62	27.22	23.62	2.09	0.49	0.20	0.45	0.18	0.13
Object 2	13.65	58.55	20.75	0.97	0.76	0.16	3.77	0.07	1.31

points. The carbide and interdendritic phases were obtained in the microstructure. The homogenization time at 1000 °C caused the refining of hard phases (Figure 5d). When homogenization time was increased, pro-eutectoid particles were distributed homogenously in the microstructure.

The microstructures of samples S4, S5 and S6 are indicated in Figures 6–8. The homogenization time was increased from 1 to 3 h and the carbides were significantly refined. Homogenization heat treatment time for sample S6 was increased up to 6 h. The microstructure of sample

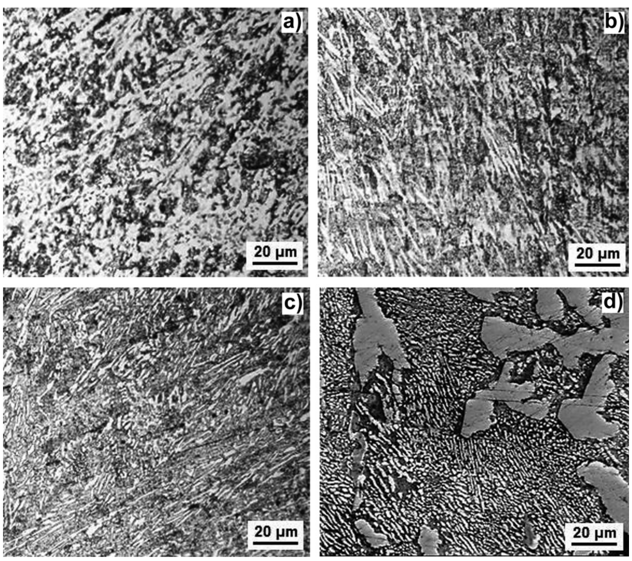

Figure 6: OM and SEM micrographs of samples, a) $S_{4.1}$, b) $S_{4.2}$, c) $S_{4.3}$, d) $S_{4.4}$.

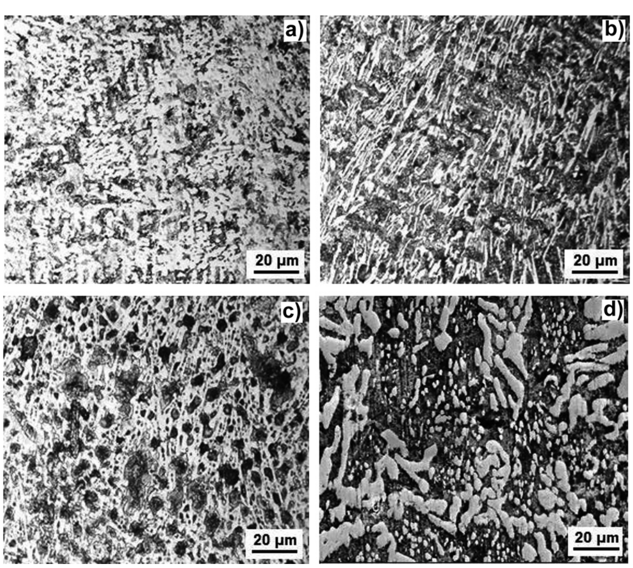

Figure 7: OM and SEM micrographs of samples, a) $S_{5.1}$, b) $S_{5.2}$, c) $S_{5.3}$, d) $S_{5.4}$.

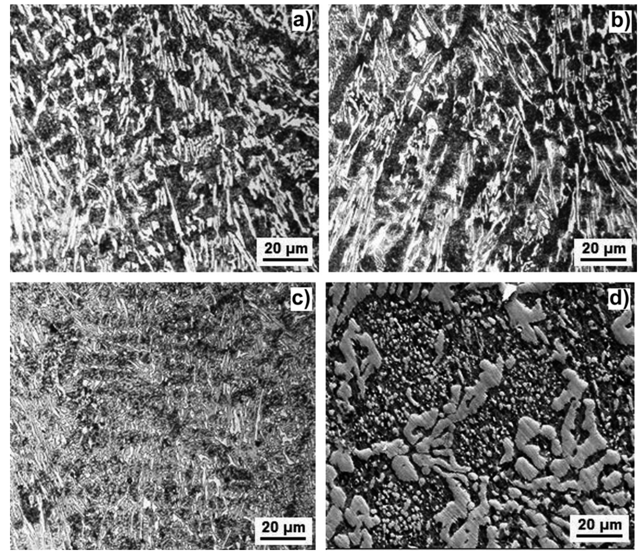

Figure 8: OM and SEM micrographs of samples, a) $S_{6.1}$, b) $S_{6.2}$, c) $S_{6.3}$, d) $S_{6.4}$.

S6 had primary carbides that were dissolved and observed in spheroid form. MC and M_2C carbides were also determined, and carbides were distributed homogenously. The microstructure of sample S6 is indicated in Figure 8. The size of the primary (M_7C_3) and secondary carbides (M_2C and MC) were identical to each other, and hard particles reduced their size to 40 μm. Titanium and chrome was found in the carbide microstructure. EDS analysis of the carbides was determined on sample $S_{2.1}$, and the results are shown in Table 3. Carbide volume ratio was associated with chemical analysis in previous studies on white cast iron [17, 18]. The chemical rate and the carbide volume varied on account of the added hard inoculant particles, which were obtained from the FeTi-FeB particulates mixture. The inoculants can change the solidification gradient throughout solidification. From the X-ray analysis results, it was determined that the carbide phase in all of these regions consisted of the primary M_7C_3 type. The heat treatment application showed that the phase hardness was reduced, and the volume ratio of carbide increased because of the decomposition of the hard phases.

The surface hardness values of samples as-cast are given in Table 4. It was also determined that the homogenization process affected hardness. The microhardness values of some carbides were greater than 2500 HV. According to the EDS analysis, these hard phases consisted of elements of Ti, C, and B. It was thought that the secondary carbides could be M_2C carbides with Mo, Ti, C and B. The primary carbides had 1700 HV microhardness values and were thought to be M_7C_3.

Table 4: Surface hardness values of samples as-cast.

No	Secondary carbide hardness (HV)	Primary carbide hardness (HV)	Hard phase ratio (vol-%)	Matrix (HV)	Surface hardness (HRC)
$S_{1.1}$	1550	–	28.4	670	45
$S_{2.1}$	1800–2000	–	30.2	800–850	40
$S_{3.1}$	2400–2500	1600–1700	33.6	800–1000	42
$S_{4.1}$	2200–2400	1500–1700	34.1	800–1000	40
$S_{5.1}$	2100–2600	1500–1700	34.2	800–1000	40
$S_{6.1}$	2000–2200	1300–1450	35.2	800–1000	54

3.2 Wear test

Figure 9a and b shows the relationship between wear rate and hardness. The abrasion rate was higher for sample S1 without FeB and FeTi. Sample S6 had a minimum wear rate. It was estimated that the reduction of the wear rate depended on the carbide size, matrix hardness, carbide hardness, and decrease of primary carbide volume in the matrix. The abrasive particle measurement played an important role in the mechanism of wear. Depending on the abrasive particle size, the abrasive particle is deformed or cut. Therefore, the ratio of the size of the reinforcement had great effect. The wear rate increased by critical carbide size, type and distribution in the microstructure. The differences in wear resistance were consistent with changes in the FeB-FeTi amount. Rough primary carbides adversely influenced the durability of HCrWCI. Consequently, it is useful to thin the microstructure to increase the strength properties of HCrWCI. FeB promotes the formation of thinned dendrites and eutectic structures [19]. The boron inoculated to the alloy contributed to the formation of a harder structure. FeTi-FeB reinforcement increased hardness and contributed to wear performance. A rise in the hardness of a thinner eutectic microstructure with 2 wt% FeTi was detected. The hardness of primary carbides was slightly reduced by the addition of FeTi. It was evident that reinforcements through inoculation resulted in a significant reduction in wear rates of the samples throughout abrasive wear tests. In other words, the samples reinforced with FeTi-FeB inoculation indicated that the inoculation rate increased and the hardness in the matrix reduced the rate of wear [20]. However, the homogenization process reduced the wear resistance (Figure 9).

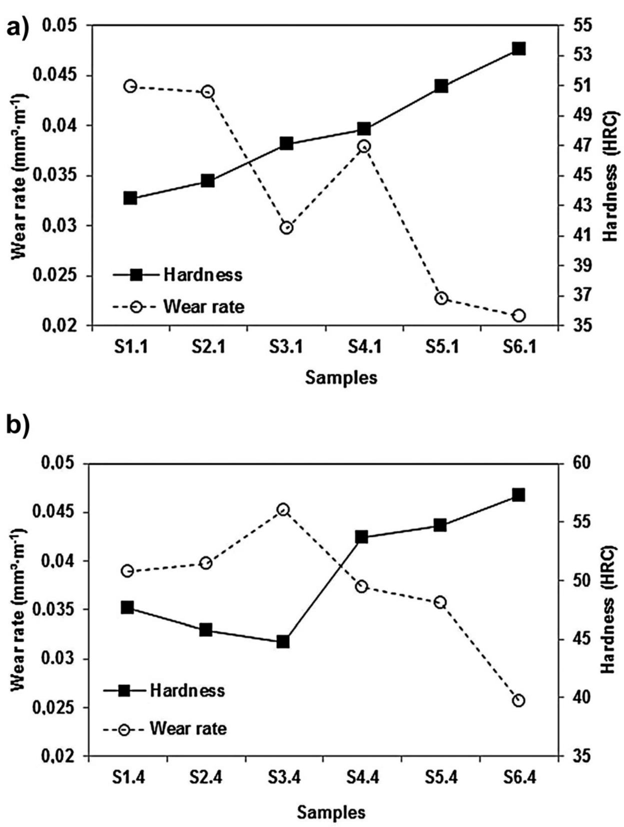

Figure 9: Relationship between wear rate and hardness for a) as-cast samples, b) heat-treated samples.

4 Conclusions

The following conclusions were reached.

- The addition of FeTi-FeB inoculants to high Cr white cast iron played an important role in the distribution of hard carbides.
- Structures having M_7C_3 carbides were surrounded by a layer of austenite and pearlitic-austenitic matrix.
- Refinement of the microstructure was related to homogenization heat treatment.
- The carbides with coarse grains decomposed and ledeburite phases were formed in the microstructure.
- A thinner microstructure improved the wear resistance of materials.
- The eutectic structure had the greatest abrasion strength and hardness due to its finer microstructure.
- The differences in wear resistance and hardness were consistent with changes in the amount of FeTi and FeB.
- FeTi-FeB reinforcement increased hardness and contributed to wear performance.

Acknowledgments: This work was supported by Domex. The authors are grateful to Domex for their assistance in conducting the experiments.
Author contributions: All the authors have accepted responsibility for the entire content of this submitted manuscript and approved submission.

Research funding: None declared.
Conflict of interest statement: The authors declare no conflicts of interest regarding this article.

References

[1] X. J. Wu, J. D. Xing, H. G. Fu, and X. H. Zhi, "Effect of titanium on the morphology of primary M_7C_3 carbides in hypereutectic high chromium white iron," *Mater. Sci. Eng. A*, vol. 457, nos. 1–2, pp. 180–185, 2007, https://doi.org/10.1016/j.msea.2006.12.006.

[2] R. J. Llewellyn, S. K. Yick, and K. F. Dolman, "Scouring erosion resistance of metallic materials used in slurry pump service," *Wear*, vol. 256, no. 6, pp. 592–599, 2004, https://doi.org/10.1016/j.wear.2003.10.002.

[3] B. Lu, J. Luo, and S. Chiovelli, "Corrosion and wear resistance of chrome white irons-a correlation to their composition and microstructure," *Metall. Mater. Trans. A*, vol. 37, pp. 3029–3038, 2006, https://doi.org/10.1007/s11661-006-0184-x.

[4] S. D. Carpenter, D. Carpenter, and J. T. H. Pearce, "XRD and electron microscope study of an as-cast 26.6% chromium white iron microstructure," *Mater. Chem. Phys.*, vol. 85, no. 1, pp. 32–40, 2004, https://doi.org/10.1016/j.matchemphys.2003.11.037.

[5] Z. L. Liu, Y. X. Li, X. Chen, and K. H. Hu, "Microstructure and mechanical properties of high boron white cast iron," *Mater. Sci. Eng. A*, vol. 486, nos. 1–2, pp. 112–116, 2008, https://doi.org/10.1016/j.msea.2007.10.017.

[6] I. Fernández and F. J. Belzunce, "Wear and oxidation behaviour of high-chromium white cast irons," *Mater. Charact.*, vol. 59, no. 6, pp. 669–674, 2008, https://doi.org/10.1016/j.matchar.2007.05.021.

[7] A. Wiengmoon, T. Chairuangsri, A. Brown, R. Brydson, D. V. Edmonds, and J. T. H. Pearce, "Microstructural and crystallographical study of carbides in 30 wt% Cr cast irons," *Acta Mater.*, vol. 53, no. 15, pp. 4143–4154, 2005, https://doi.org/10.1016/j.actamat.2005.05.019.

[8] A. Bahrami, S. H. M. Anijdan, M. A. Golozar, and M. Shamanian, "Effects of conventional heat treatment on wear resistance of AISI H13 tool steel," *Wear*, vol. 258, nos. 5–6, pp. 846–851, 2005, https://doi.org/10.1016/j.wear.2004.09.008.

[9] A. Bedolla-Jacuinde, "Microstructure of vanadium-niobium- and titanium alloyed high-chromium white cast irons," *Int. J. Cast Metals Res.*, vol. 13, no. 6, pp. 343–361, 2001, https://doi.org/10.1080/13640461.2001.11819416.

[10] R. K. Galgali, H. S. Ray, and A. K. Chakrabarti, "Wear characteristics of TiC reinforced cast iron composites. Part 1. Adhesive wear," *Mater. Sci. Technol.*, vol. 14, no. 11, pp. 810–815, 1998, https://doi.org/10.1179/mst.1998.14.8.810.

[11] Y. H. Qu, J. D. Xing, X. Zhi, J. Peng, and H. Fu, "Effect of cerium on the as-cast microstructure of a hypereutectic high chromium cast iron," *Mater. Lett.*, vol. 62, nos. 17–18, pp. 3024–3027, 2008, https://doi.org/10.1016/j.matlet.2008.01.129.

[12] X. Chen and Y. X. Li, "Effect of heat treatment on microstructure and mechanical properties of high boron white cast iron," *Mater Sci Eng A*, vol. 528, no. 2, pp. 770–775, 2010, https://doi.org/10.1016/j.msea.2010.09.092.

[13] X. H. Zhi, J. D. Xing, G. Yimin, F. Hanguang, P. Jiyun, and X. Bing, "Effect of heat treatment on microstructure and mechanical properties of a Ti-bearing hypereutectic high chromium white cast iron," *Mater Sci Eng A*, vol. 487, nos. 1–2, pp. 171–179, 2009, https://doi.org/10.1016/j.msea.2007.10.009.

[14] C. Scandian, C. Boher, J. D. B. De Mello, and F. Rezai-Aria, "Effect of molybdenum and chromium contents in sliding wear of high-chromium white cast iron: the relationship between microstructure and wear," *Wear*, vol. 267, nos. 1–4, pp. 401–418, 2009, https://doi.org/10.1016/j.wear.2008.12.095.

[15] M. Mohammadnezhad, V. Javaheri, M. Shamanian, M. Naseri, and M. Bahrami, "Effects of vanadium addition on microstructure, mechanical properties and wear resistance of Ni-Hard4 white cast iron," *Mater. Des.*, vol. 49, pp. 888–893, 2013, https://doi.org/10.1016/j.matdes.2013.02.043.

[16] Z. Xiaohui, X. Jiandong, F. Hanguang, and X. Bing, "Effect of niobium on the as-cast microstructure of hypereutectic high chromium cast iron," *Mater. Lett.*, vol. 62, nos. 6–7, pp. 857–860, 2008, https://doi.org/10.1016/j.matlet.2007.06.084.

[17] T. Teker and S. O. Yılmaz, "Effect of carbides on wear resistance of white cast iron alloyed with 12.7 wt% Cr and nickel," *Mater. Test.*, vol. 62, no. 8, pp. 788–792, 2020, https://doi.org/10.3139/120.111552.

[18] R. J. Chung, X. Tang, D. Y. Li, B. Hinckley, and K. Dolman, "Effects of titanium addition on microstructure and wear resistance of hypereutectic high chromium cast iron Fe–25wt%Cr–4wt%C," *Wear*, vol. 269, nos. 1–4, pp. 356–361, 2009, https://doi.org/10.1016/j.wear.2008.12.061.

[19] T. Teker, S. Karataş, and S. O. Yılmaz, "Microstructure and wear properties of AISI 1020 steel surface modified by HARDOX 450 and FeB powder mixture," *Protect. Met. Phys. Chem. Surface*, vol. 50, pp. 94–103, 2014, https://doi.org/10.1134/S2070205114010213 94.

[20] Z. Mei, Y. W. Yan, and K. Cui, "Effect of matrix composition on the microstructure of *in situ* synthesized TiC particulate reinforced iron-based composites," *Mater. Lett.*, vol. 57, no. 21, pp. 3175–3181, 2003, https://doi.org/10.1016/S0167-577X(03)00020-X.

The authors of this contribution

Tanju Teker
Prof. Dr. Tanju Teker, born in 1971, works at the University of Sivas Cumhuriyet, Faculty of Technology, Department of Manufacturing Engineering, Sivas, Turkey. He graduated in Metallurgy Education from Gazi University, Ankara, Turkey, in 1997. He received his MSc and PhD degrees from Firat University, Elazig, Turkey in 2004 and 2010, respectively. He studied metal coating techniques, fusion and solid state welding methods, casting and wear.

S. Osman Yilmaz
Prof. Dr. S. Osman Yilmaz, born in 1966, works at the University of Namık Kemal, Faculty of Engineering, Department of Machine Engineering, Corlu, Tekirdağ, Turkey. He received his BSc from the University of METU, Faculty of Engineering, Metallurgy and Materials Engineering Department in 1989, his MSc from the Institute of Science and Technology, Metallurgy Department in 1992 and his Ph.D from the University of Firat, Institute of Science and Technology, Metallurgy

Department, Elazig in 1998. He studied metal coating techniques, surface modification, welding, casting and wear.

İ. Savaş Dalmiş

Assist. Prof. Dr. İ. Savaş Dalmiş, born in 1975, works at the University of Namık Kemal, Corlu, Tekirdağ in Turkey. He received his BSc from the Teacher Training in Machine Department, Faculty of Technical Education, University of Marmara, Istanbul, Turkey, in 1997, his MSc from the Agricultural Machinery of the Institute of Science, University of Trakya, Edirne, Turkey in 2000 and his PhD from the Agricultural Machinery Department, Institute of Science, University of Trakya, Edirne, Turkey in 2006. His research interests include Machine design, mechatronics system design, manufacturing technologies, Cad/Cam systems, tool designs and welding technologies.